Chemistry Europe
European Chemical Societies Publishing

Synthesis and Hydrogen-Bond Patterns of Aryl-Group Substituted Silanediols and -triols from Alkoxy- and Chlorosilanes

Jan-Falk Kannengießer,[a] Max Briesenick,[a] Dennis Meier,[a] Volker Huch,[a] Bernd Morgenstern,[a] and Guido Kickelbick*[a]

Dedicated to Professor Ulrich Schubert on the occasion of his 75th birthday

Abstract: Organosilanols typically show a high condensation tendency and only exist as stable isolable molecules under very specific steric and electronic conditions at the silicon atom. In the present work, various novel representatives of this class of compounds were synthesized by hydrolysis of alkoxy- or chlorosilanes. Phenyl, 1-naphthyl, and 9-phenanthrenyl substituents at the silicon atom were applied to systematically study the influence of the aromatic substituents on the structure and reactivity of the compounds. Chemical shifts in ^{29}Si NMR spectroscopy in solution, correlated well with the expected electronic situation induced by the substitution pattern on the Si atom. ^{1}H NMR studies allowed the detection of strong intermolecular hydrogen bonds. Single-crystal X-ray structures of the alkoxides and the chlorosilanes are dominated by π-π interactions of the aromatic systems, which are substituted by strong hydrogen bonding interactions representing various structural motifs in the respective silanol structures.

Introduction

The first stable silanol, triphenylsilanol, was already isolated and studied by Ladenburg as early as 1871.[1] The isolation of stable organosilanediols succeeded already decades ago with the single-crystal structures of diethylsilanediol,[2] and diallylsilanediol.[3] The most commonly known disilanol is most likely diphenylsilanediol.[4–7] The first structural description of a silanetriol, namely cyclohexylsilanetriol, was published in 1982 by Ishida et al.[8] But reasonably stable silanetriols such as phenylsilanetriol were already synthesized earlier.[7,9]

Silanols are mostly synthesized by the hydrolysis of their corresponding alkoxy or chloro derivatives, but other synthetic methods such as the oxidation of a Si–H bond were also applied.[10] The unique properties of silanols were the basis of their use as precursors for polymers[11–16] and polyhedral oligomeric silsesquioxanes,[17,18] as silicon based surfactants,[19] as protease inhibitors,[20,21] as cross-coupling agents,[22,23] as systems for anion detection,[24] and as agents for surface functionalization.[25–30] Some of the previously mentioned applications are based on the strongly developed ability of silanols to form very strong hydrogen bonds, which is based on the hydrogen bond acidity coupled with the simultaneously very high hydrogen bond basicity.[31,32] The relatively low pK_a values compared to the corresponding carbinols are a consequence of the high acidity. They were determined for a few silanols such as Et_3SiOH (13.63),[31] Ph_3SiOH (16.57–16.63),[33] $PhC{\equiv}CSiMe_2OH$ (9.8)[34] and *m*-$ClC_6H_4SiMe_2OH$ (11).[34] The high tendency of the silanols to form strong hydrogen bonds is represented by the formation of a variety of structural motifs in the crystalline state.[25,31,35] The structural motifs of the silanols in the solid state depend on the substituents on the silicon on the one hand[31,32] and on the solvent used for crystallization on the other.[36] Known crystalline structural hydrogen bonding motifs in this context are, for example, bilayer[8] and tubular structures,[37] as well as various oligomeric structures, such as dimers,[38] tetramers[39] or hexamers[4] (Figure 1). Using the example of *tert*-butyl silanetriol, Pietschnig and coworkers showed that silanols in solution also form hydrogen bond supported aggregates.[40] Theoretical calculations suggest that *tert*-butyl silanetriol forms dimers even in the gas phase. However, this assumption could not be confirmed due to the high temperature required for measurement.[41]

In the present work, we have synthesized silanediols and -triols with systematic variations of the (poly)aromatic substitution patterns at the silicon atom. The influence of the substituents on the reactivity regarding the hydrolysis of alkoxysilanes was investigated. The objective was to derive structure-property relationships for the hydrolysis, stability, and

[a] J.-F. Kannengießer, M. Briesenick, Dr. D. Meier, Dr. V. Huch, Dr. B. Morgenstern, Prof. Dr. G. Kickelbick
Inorganic Solid-State Chemistry
Saarland University
Campus, Building C4 1, 66123 Saarbrücken (Germany)
E-mail: guido.kickelbick@uni-saarland.de

Supporting information for this article is available on the WWW under https://doi.org/10.1002/chem.202102729

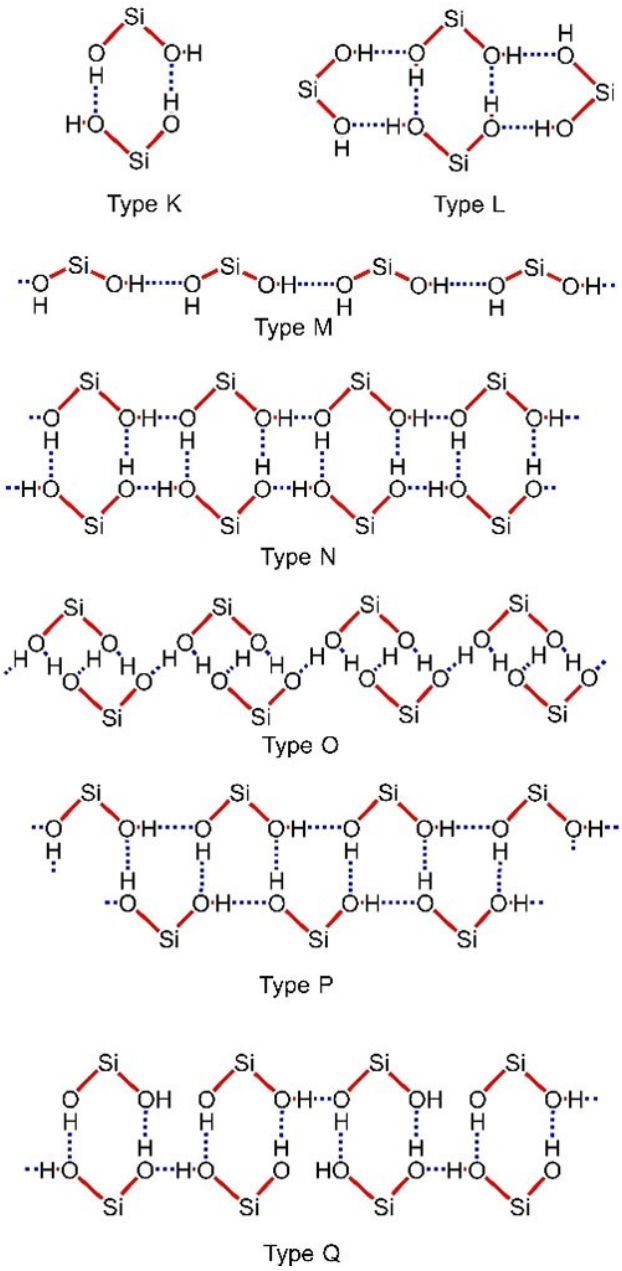

Figure 1. Hydrogen bond supported structural motifs in silanediols.[32]

intermolecular hydrogen bonding interactions of various silanols. Thus, this work has similarities to previous works where the substituents were also systematically varied.[42] In future studies, the obtained results should enable a new synthetic route for a step-by-step assembly of polysiloxanes and polysilsesquioxanes.

Results and Discussion

Starting compounds for the preparation of the silanols were alkoxy- or chlorosilanes. The compounds with variations in substitution patterns on the Si atoms were synthesized applying nucleophilic substitution reactions starting from the respective Grignard reagents and the corresponding methoxysilanes as electrophiles in THF. Purification of the resulting compounds was carried out by distillation or washing with n-hexane at low temperatures. The dichlorodi(naphthalen-1-yl)silane (**6c**) was obtained by a lithiation of the 1-bromonaphthalene and subsequent reaction with tetrachlorosilane. The organochlorosilane was purified by recrystallization from toluene. Both reaction pathways are shown in Scheme 1.

This approach allowed us to synthesize a variety of mono and diaromatic substituted silicon compounds (Figure 2), which were studied as precursors for silanols. For reasons of comparison we included in our discussions the dimethoxy(methyl)(phenyl)silane (**1a**), dimethoxydiphenylsilane (**2a**), and diphenylsilanediol (**2b**)[4–7] which are commercially available derivates.

^{1}H NMR spectra and elemental analysis of the prepared non-hydrolysed compounds proved a successful synthesis and clean products. As expected, the synthetic yield of the alkoxides correlates with the steric hindrance at the Si atom. Generally, if a methyl group is present yields are higher compared to systems with two aromatic substituents. ^{29}Si NMR spectra revealed only one sharp signal in each case with chemical shifts ranging from −52.70 to 7.62 ppm (Figure 8), which also verified the purity of the compounds. FTIR spectra supported the NMR results. The most intense vibrations in the spectra result from the methoxy groups at about 1070 cm^{-1}, the aromatic C–H vibration at about 700 cm^{-1}, and the characteristic Si–O vibration at about 800 cm^{-1} (Figure 11).

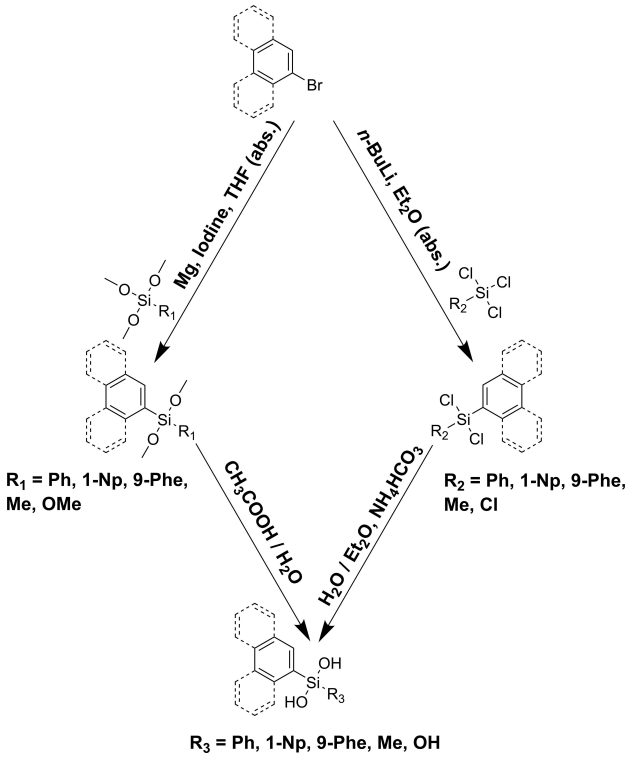

Scheme 1. Synthesis scheme for the preparation of alkoxy- or chlorosilanes and the subsequent hydrolysis for the formation of silanols.

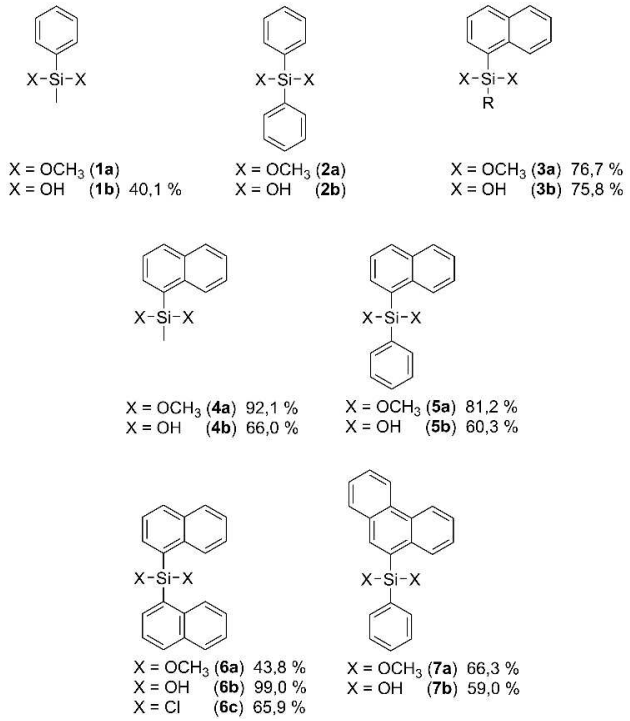

Figure 2. Structural formulas of all compounds considered with their corresponding abbreviations and yields obtained. Compounds **1a**, **2a** and **2b** are commercially available.

Several obtained molecular compounds crystallized, and we were able to study their structures by single-crystal X-ray structure analysis. Compounds **3a**, **6a**, and **6c** crystallize in a monoclinic crystal system, compound **4a** crystallizes in a triclinic crystal system, and compound **7a** crystallizes in an orthorhombic crystal system. The most important bond lengths and angles as well as other crystalline parameters are listed in Table 1. Compounds **1a** and **2a**, and **4a** are liquids and therefore no structural information could be obtained applying X-ray single-crystal analysis.

Table 1. Summary of important parameters of alkoxy- and chlorosilane crystal structures.

Compound	**3a**	**5a**	**6a**	**6c**	**7a**
Crystal system	mono-clinic	triclinic	mono-clinic	mono-clinic	ortho-rhombic
Space group	$P2_1/c$	$P\bar{1}$	$I2/a$	$P2_1/n$	$Pbca$
d (Si–O_1(Cl_1)) [pm]	162.82	163.04	163.71	206.10	163.12
d (Si–O_2(Cl_2)) [pm]	161.79	163.00	–	205.91	162.81
d (Si–O_3) [pm]	163.03	–	–	–	–
d (Si–$C_{1/4}$) [pm]	185.45	186.50	186.88	184.86	186.51
d (Si–$C_{11/15}$) [pm]	–	185.64	–	186.03	185.58
∢ (Ar–Si–Ar) [°]	–	111.39	113.57	117.04	113.37
∢ ((Cl)O–Si–O(Cl)) [°]	112.57	107.45	111.13	111.30	110.93
$\measuredangle_{Tors}$ (Ar–Si–Ar) [°]	–	89.01	87.37	62.10	87.18
d (Y-shaped-π-π) [pm]	–	486.8; 500.6	485.1	–	487.3; 490.9
d (parallel-stacking-π-π) [pm]	–	–	–	392.2	–
∢ (π-π-inter-actions) [°]	–	89.01	87.37	10.69	80.12; 86.42

The three-dimensional crystal structures of the obtained alkoxides and chlorosilanes are dominated by the intermolecular π-π interactions of the aromatic systems with typical structural motifs. Compound **3a**, whose crystal structure is known from literature,[43] is an exception (Figure 3). Bond lengths and angles around the Si atom are in the range of the typical values of similar structures.[43] Typically molecular structures with polycyclic aromatic substituents show structural motifs which are based on interactions of the substituents. But compound **3a** does neither display the so-called "parallel stacking" pattern, nor T-shaped or Y-shaped patterns.[44,45] A recent study revealed that weak C–H-π bonds are present in the crystal structure of this compound.[43]

The dialkoxysilane **5a** (Figure 4) reveals bond lengths and angles around the Si atom comparable to the other dimethoxysilanes (**6a**; **7a**) (Table 1) and agrees well with literature-known dimethoxysilanes such as bis[3,4,5,6-tetrakis (trimethylsilyl)cyclohexen-1-yl]dimethoxysilanes[46] or dimethoxybis(N-methylpyrrol-2-yl)silanes.[47] The crystal structure of compound **5a** reveals so-called "perpendicular Y-shaped" intermolecular π-π interactions between the phenyl and the naphthyl groups.[45] This means that the aromatic rings are not parallel but perpendicular to each other, with the edge of a phenyl ring being perpendicular to a naphthyl ring in each case (edge-to-face interactions).[45,48] The angle between the rings is 89.01°. The distance between the naphthyl ring plane and the

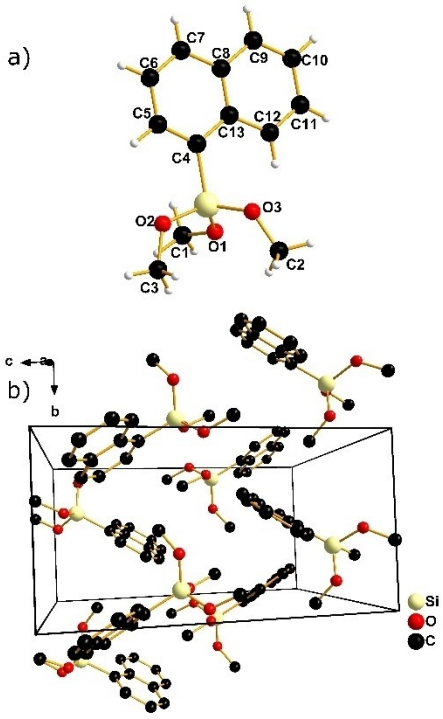

Figure 3. a) Illustration of the 3D structure of **3a**. b) Unit cell in the crystal structure of compound **3a**.[43]

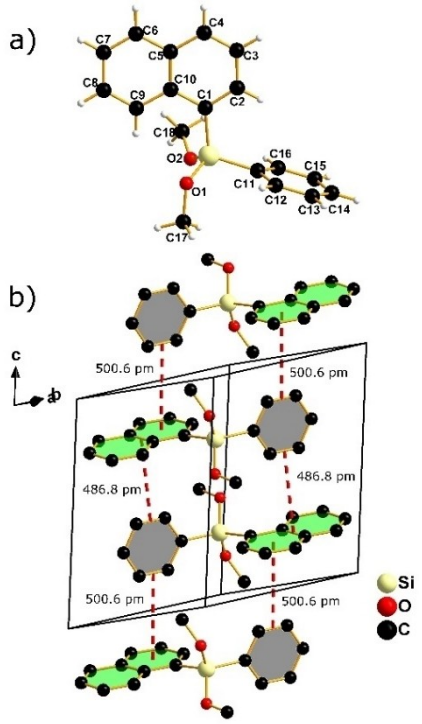

Figure 4. a) Single-crystal structure of compound **5a** (CCDC 2093388). b) Illustration of the unit cell with Y-shaped π-π interactions, measured from centre to centre, highlighted (red).

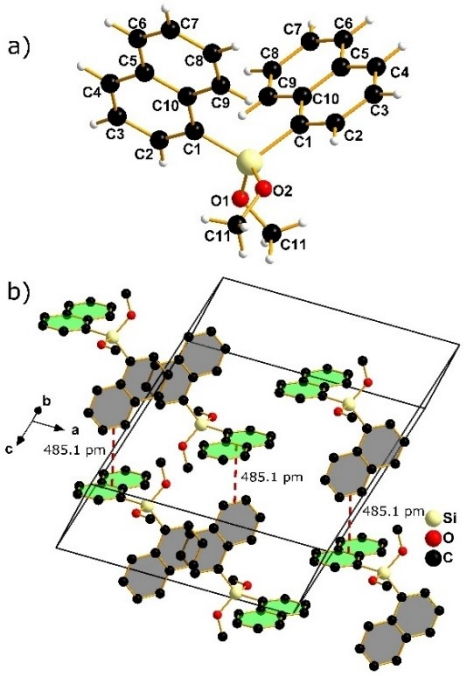

Figure 5. a) Single-crystal structure of compound **6a** (CCDC 2093389). b) Illustration of the unit cell with Y-shaped π-π interactions, measured from centre to centre highlighted (red).

centre of the phenyl ring perpendicular to it is 486.8 pm and 500.6 pm, respectively.

Dimethoxysilane **6a** shows the expected tetrahedral surrounding of the Si atom including the expected bond lengths and angles.[46,47] A "Y-shaped" π-π interaction formed between the naphthyl groups is observed in the three-dimensional structure (Figure 5). The respective angle of these edge-to-face interactions between the two naphthyl groups is 87.37°.[45,48] The distance from the plane to the centre of the nearest phenyl ring is 485.1 pm and is very similar to compound **5a**.

Compound **6c** reveals "parallel stacking" π-π interactions (Figure 6).[49,50] However, the aromatic rings deviate slightly from perfect parallelism, as an angle of 10.69° is found between them. In addition, the aromatic rings are shifted against each other, since repulsive interactions would otherwise occur.[45] The distance between the centres of the naphthyl groups is 392.2 pm.[44] Interestingly, the distance between the two naphthyl groups is larger than described in the literature.[49–51]

Y-shaped π-π interactions are also observed in the crystal structure of alkoxysilane **7a** (Figure 7). Here, a phenanthrenyl group alternately interacts with another phenanthrenyl group and a phenyl group with a phenanthrenyl group. The angle between the phenanthrenyl groups is 80.12°. The distance between the aromatic plane and the centre of the nearest phenyl ring of the phenanthrenyl group is 490.9 pm. This distance is consistent with the molecules considered previously and with the literature for benzene molecules (470 pm–492 pm).[44] The angle between the phenyl group and the

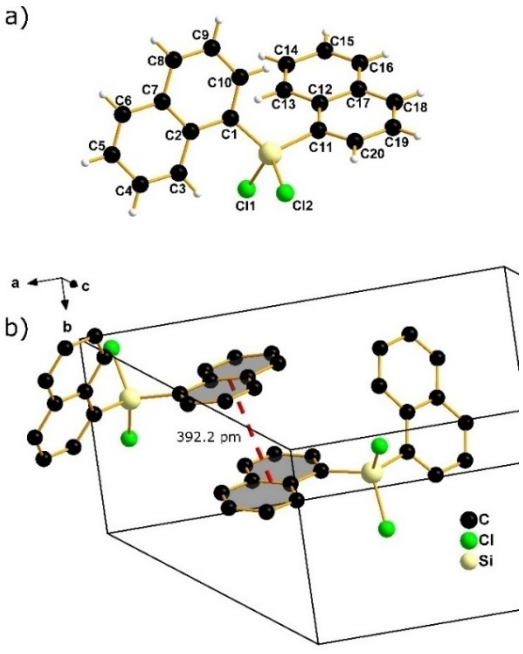

Figure 6. a) Single-crystal structure of compound **6c**. b) Illustration of the unit cell showing sandwich π-π interactions measured from centre to centre (red).[49–51]

phenanthrenyl group in the second π-π interaction is 86.42°. The distance between the phenanthrenyl plane and the centre of the phenyl group is 487.3 pm. This is again larger than the

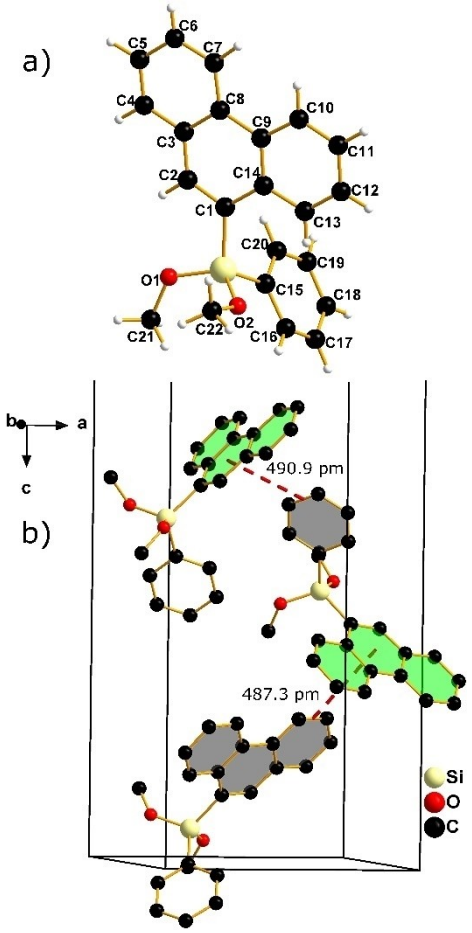

Figure 7. a) Single-crystal structure of compound **7a** (CCDC 2073539). b) Illustration of the unit cell with Y-shaped π-π interactions, measured from centre to centre marked in red.

phenanthrenyl-phenanthrenyl distance and is also closer to the above values and to the literature values.[44]

In summary the crystalline structures of the alkoxy and chlorosilanes are dominated by π-π interactions. No trend between the bond angles of aryl groups (111.39°–117.04°) or oxygen or chlorine atoms (107.45°–111.30°) and the substitution pattern could be found (Table 1). Furthermore, no trend for the torsion angles between the aromatic planes (62.10°–89.01°) was observed. But values are much smaller for the chlorosilane **6c** than for the alkoxysilanes. The π-π interactions, which occur in compounds **5a**, **6a** and **7a**, are Y-shaped-π-π interactions with similar distances (485.1 pm–500.6 pm) and angles (80.12°–89.01°). The chlorosilane **6c** shows parallel-stacking-π-π interactions with a spacing of 392.2 pm between aromatic planes and a tilt angle of 10.69°. The only compound that does not exhibit any π-π interactions is the trialkoxysilane **3a**.

The silanols (Figure 2 (**1b**–**7b**)) were all obtained by hydrolysis of the precursor compounds presented (Scheme 1). In all cases, we tried to perform hydrolysis of the methoxysilanes, since they are significantly more stable compared to the corresponding chlorosilanes. In the case of chlorosilanes, humidity can cause hydrolysis with the formation of hydrochloric acid, which can catalyse a subsequent condensation reaction. Controlled hydrolysis was carried out under acidic conditions in order to favour hydrolysis over condensation compared to basic conditions.[52,53] Acetic acid as a weak acid was applied for hydrolysis because stronger acids, such as hydrochloric acid, can catalyse the condensation reactions. Variations of the acid concentration during hydrolysis allow for a better matching of the reactivity of the organoalkoxysilane. The reaction conditions (temperature, acid concentration) were chosen as mild as possible to suppress subsequent condensation of the resulting silanols as a side reaction. To remove oligomeric and polymeric compounds, the silanols were washed with cold toluene for purification. The reactivity of the precursors towards hydrolysis is influenced by the electronic as well as steric effects on the Si atom.[53–55]

Hydrolysis of the alkoxysilanes gave yields ranging from about 40% (**1b**) to 75.8% (**3b**). In the case of compound **6b**, hydrolysis of the corresponding alkoxysilane was not successful. Even at very high acetic acid concentrations, no hydrolysis took place, which is why the more reactive chlorosilane was used as the starting compound. In this case, water was sufficient for hydrolysis, but an acid scavenger (NH_4HCO_3) had to be used to intercept the hydrochloric acid formed during hydrolysis and thus prevent acid-catalyzed condensation. An almost quantitative yield (99%) was obtained in this reaction.

Complete hydrolysis can be determined in the ^{29}Si NMR spectrum because the signals of the silanols are always high field-shifted compared to the alkoxy- or chlorosilanes (Figure 8). The substituents on the Si atom essentially determine the chemical shift in the ^{29}Si NMR spectrum. Electron-donating substituents increase the electron density and thus the shielding at the silicon atom which results in a high-field shift. In contrast, electron-withdrawing substituents have a shielding effect.

In the compounds investigated in our study, the positive mesomeric effect of the aryl groups clearly exceeded the positive inductive effect of the methyl groups, which is why methyl-containing compounds are more strongly low-field shifted than aryl compounds (Figure 8).[56] The mesomeric effect of the oxygen atoms bonded to the silicon is even stronger than that of the organic substituents, which is why compounds **3a/b** are the only trialkoxysilane or silanetriol that are significantly more high-field shifted than the dialkoxysilanes or silanediols, respectively. In the literature, ^{29}Si NMR data are often not cited. However, the trend we observed agrees well with similar compounds in which two or three oxygen atoms are bonded to the silicon atom.[32] As an example, the silanetriol $TipSi(OH)_3$ shows a chemical shift of 52.3 ppm,[57] while the silanediol $(HO)_2MeSiC_6H_4SiMe(OH)_2$ reveals a chemical shift of −21.3 ppm, which shows the large general difference in the chemical shift of a silanetriol compared to a silanediol. Another comparable system is di-(9-anthryl)silanediol, which has a ^{29}Si NMR shift of −23.7 ppm.[24]

Probably the most comparable of the proprietary silanols is compound **6b** revealing a chemical shift of 30.9 ppm in the ^{29}Si NMR. The deviation of the shifts can be explained by the variations in the substitution pattern. Compounds **2a/b**, **5a/b**,

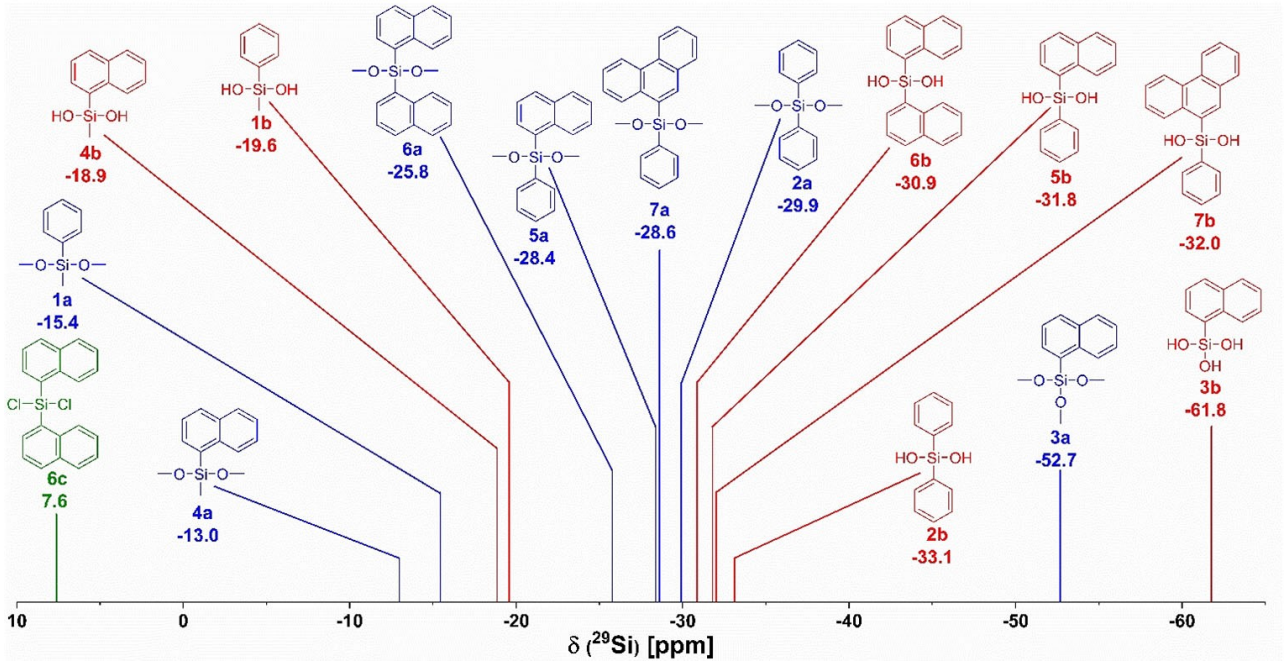

Figure 8. Graphical representation of the ^{29}Si NMR chemical shifts in a acetone-d_6 solution of the compounds . Here, the silanols are marked red, the corresponding alkoxysilanes blue, and the chlorosilane green. Below the structural formulas of the compounds are the abbreviations and the exact chemical shifts in the ^{29}Si NMR spectrum in ppm.

and **7a/b** are very comparable in terms of their substituents, since only one of the aromatic substituent changes. The following order of the three polyaromatic substituents was found with respect to the chemical shift in the ^{29}Si NMR: 1-naphthyl > 9-phenanthrenyl > phenyl. At least the higher shift of the naphthyl group with respect to the phenyl group is also reported in the literature.[49]

As mentioned above, the alkoxy- or chlorosilane is always more downfield-shifted in the ^{29}Si NMR spectrum than the corresponding silanol. This trend can be observed for all compounds represented in this study (Figure 8). Since the organic substituents are the same in these groups, the hydroxyl group and the methoxy group can be compared regarding their electronic effects. Both groups exert a positive mesomeric effect on the silicon atom via the free electron pairs of the oxygen atom. The hydroxyl group has a stronger ionic character and thus the oxygen atom in the hydroxyl group has a lower electron withdrawing effect than the methoxy group, resulting in a high-field shift.,[58] which is also described in literature for the system $PhSiMe(OEt)_2$. In this previous work the ^{29}Si signal shifted from −17.6 ppm for the alkoxysilane to −18.2 ppm for the corresponding silanediol.[58]

In the ^{1}H NMR spectra the presence of silanol groups can be identified by a new peak in about 6 ppm. NMR spectroscopy can thus be used to follow the hydrolysis of alkoxysilanes. As one example compound **1a** (Figure S1 in the Supporting Information) was used and the conversion of methoxy groups to hydroxy groups was studied. The hydrolysis of compound **1a** was carried out under very mild conditions. Figure 9 shows complete hydrolysis after approx. 60 min at 0 °C and an acetic acid concentration of 1 wt%. Hydrolysis of the remaining alkoxysilanes required more time, higher temperatures and/or increased acid concentrations.

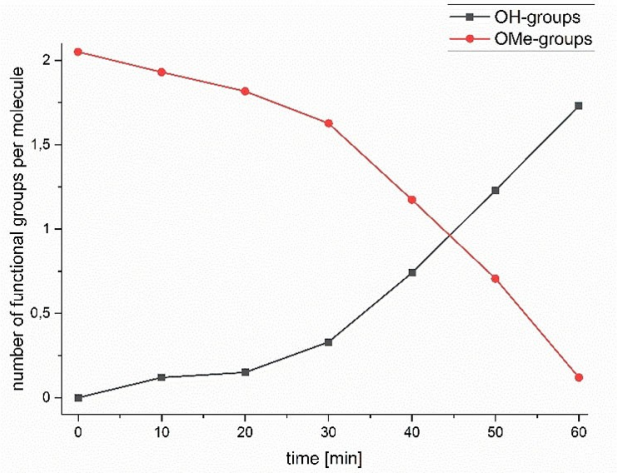

Figure 9. Representation of the time-dependent reaction progress in the synthesis of **1b**.

Based on the hydrolysis curve (Figure 9), statistically the hydrolysis of the first methoxy group takes significantly longer than that of the second methoxy group. Most likely steric factors, electronic factors, and improved solubility of the partially hydrolysed species are responsible for this behaviour.[59] The chemical shift of the silanol group in the ^{1}H NMR spectrum, which was only visible in solvents that can form hydrogen bonds, varies greatly within the series of silanols

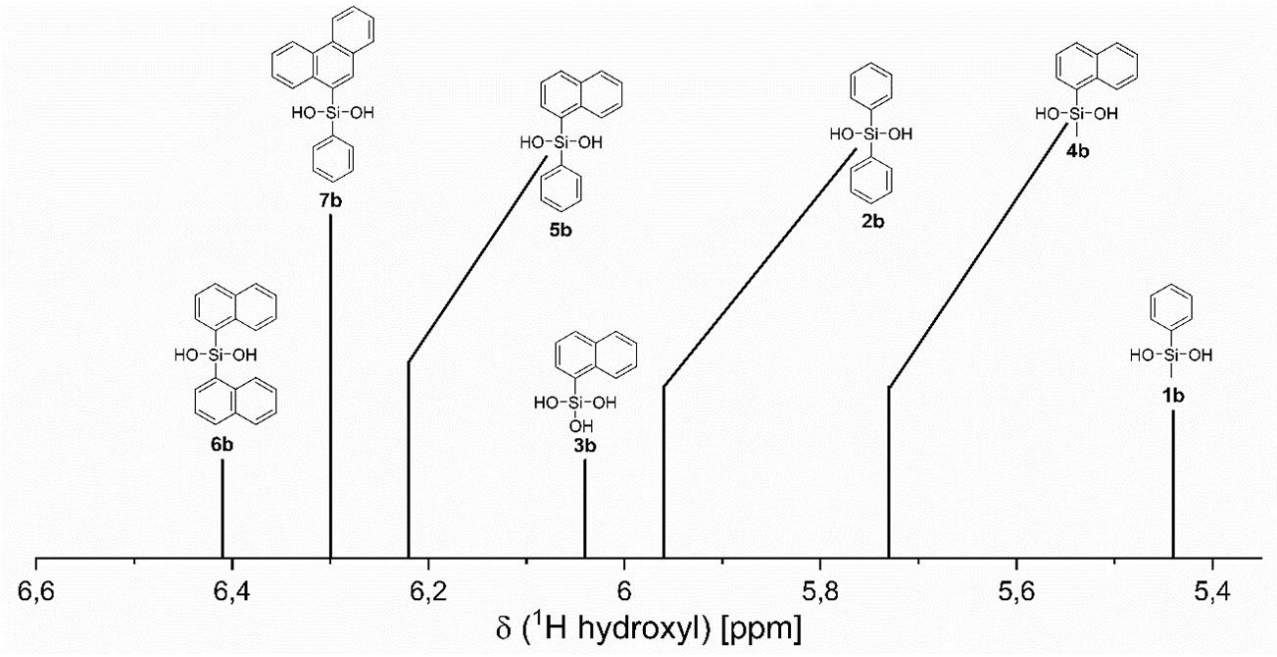

Figure 10. Chemical shifts of the silanol group in the ^{1}H NMR spectrum, measured in acetone-d_6.

considered and is in the range of 5.4–6.4 ppm for acetone-d_6 (Figure 10).

Thus, the chemical shift of the silanol group in the ^{1}H NMR should follow the same trend as the shift of the silicon atoms in the ^{29}Si NMR spectrum. However, the observed trend of the two spectroscopic methods varies (Figure 10). The experimentally found order of the compounds cannot be explained by the electronic effects discussed above. The changed order of the compounds is preserved when measured in different solvents. In fact, a trend emerges in which methyl groups on the Si atom probably provide a high-field shift and aryl substituents provide a low-field shift in comparison. However, the results of the ^{29}Si NMR spectroscopic studies showed the exact opposite for the silicon atom, where the aryl substituents caused a high-field shift compared to the methyl group. This argues against a sole influence of the chemical shift of the silanol protons by the substituents bound to silicon. According to the above theory, the most strongly shielded silanols in the ^{29}Si NMR spectrum (Figure 8) should also have the most strongly shielded silanol groups in the ^{1}H NMR spectrum, which is not the case. Another effect, like a solvent effect caused by hydrogen bonding of the solvents to the silanol, must therefore have a much greater influence. In general, the formation of a hydrogen bond leads to a low field shift in the ^{1}H NMR.[60,61] The strength of the hydrogen bond and thus the strength of the shift of the silanol proton depend on the substituents on the silicon atom. Electronic effects and probably steric effects also play a role. It has been shown in the literature[32,62] that arylsilanols are stronger hydrogen bond donors than alkylsilanols, which leads to a low-field shift of the silanol signal (Figure 10).

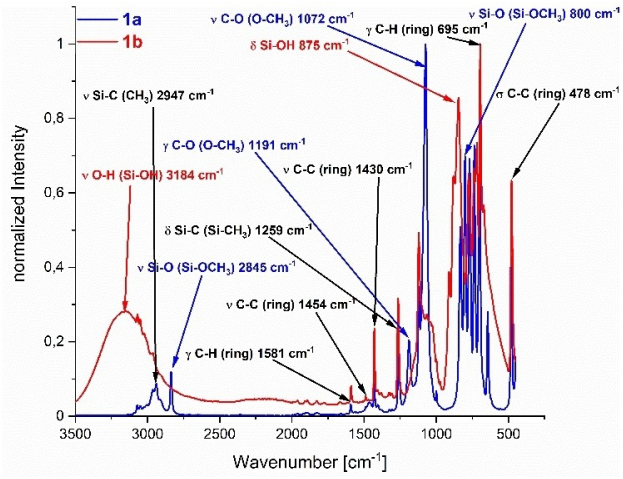

Figure 11. FTIR spectrum of **1a** (blue) and **1b** (red). These were measured as solid or liquid compound using an ATR array.

Hydrogen bonding abilities were investigated by ^{1}H NMR of the silanols in different solvents. The signal of the Si–OH varies strongly with the solvent, which can be seen in Table 2. The most shielded silanol groups were observed in acetone-d_6, while the more deshielded ones were obtained in DMSO. This observation can be explained based on the stronger hydrogen bonds to DMSO, which can be quantified with the pK_{HB} values (DMSO: 2.58; acetone: 1.18).[63] Due to solubility problems of the compounds in D_2O we tested the effect of water by adding small amounts of water (20 μL) to a solution of the compounds in acetone-d_6. According to the literature,[63] the pK_{HB} value of water (0.64) and thus the strength of the resulting hydrogen bonds, is significantly lower than that of acetone and DMSO.

Table 2. ^{1}H NMR signals of the hydroxyl group of all silanols measured in different media.

Compound	^{1}H shift in acetone-d_6 [ppm]	^{1}H shift in acetone-d_6 with 20 µL H_2O [ppm]	^{1}H shift in DMSO-d_6 [ppm]
1b	5.44	5.73	6.35
2b	5.96	6.31	6.96
3b	6.04	6.38	6.88
4b	5.73	5.99	6.63
5b	6.22	6.50	7.21
6b	6.41	6.68	7.42
7b	6.3	6.61	7.31

However, the low-field shift suggests the exact opposite (Table 2).

Interestingly, ^{29}Si NMR spectra of the silanols in DMSO-d_6 show a high-field shift of about 1–3 ppm compared to the spectra in aceton-d_6. For example, compound **4b** shows a chemical shift of −21.1 ppm in DMSO, which is 2.2 ppm less than in aceton-d_6. Compound **5b** (−33.8 ppm) and compound **6b** (−33.3 ppm) as well as all other silanols also show these properties. Thus, this behavior is exactly opposite to the behavior in the ^{1}H NMR spectra. However, it is not easy to find an explanation for this observation. It is conceivable that the previous covalent O–H bond is weakened by the stronger hydrogen bonds due to the use of DMSO instead of acetone, which slightly increases the electron density at the oxygen atom and thus also at the silicon atom. As a result, the silicon atom is somewhat more strongly shielded, which leads to a shift to a higher field.

ATR-FTIR spectroscopy also allows a reaction control and structure elucidation. We only show here exemplary the FTIR spectra of compounds **1a** and **1b** (Figure 11). The spectra of the other compounds are very similar to those shown below. The asymmetric C–H stretching vibration at 2947 cm^{-1} from the methyl group can be observed in both compound classes.[64] The aromatic groups revealed the typical C–H vibrations at 1581 cm^{-1}, the C–C stretching vibration at 1454 cm^{-1}, and the C–C vibration at 478 cm^{-1}.[64–66] The various synthesized alkoxysilanes and silanols differ only slightly in their FTIR spectra. A special vibration that only occurs in compounds **1a/b** and **4a/b** is the Si-C spreading vibration at 1259 cm^{-1}, which is caused by the methyl group attached to the silicon atom.

Specific vibrational bands revealing the hydrolysis are the O–H stretching vibration of the silanol group, for compound **1b** the peak maximum is located at 3184 cm^{-1}, and the Si–OH spreading vibration located at 875 cm^{-1} (Figure 11 red).[65,67] The very broad O–H stretching vibration partially covers the asymmetric C–H stretching vibration at 2947 cm^{-1}. To emphasise the corresponding vibration range, an enlargement was chosen for all synthesised alkoxysilanes and silanols (Figure 12), which shows the superposition of the C–H stretching oscillations and the OH-group vibrations. It has been shown in the literature that the O–H stretching vibration of a "free" hydroxyl group, i.e. without hydrogen bonds, is very similar (3620–3695 cm^{-1}) even for strongly differing silanols.[32] The observed broad O–H stretching vibration of the investigated silanols is found at significantly lower wavenumbers (3154–3353 cm^{-1}). This shift to lower wavenumbers has often been described in the literature[31,32,62,68,69] and indicates hydrogen bonding in the solid. In the case of the silanediol ArN(SiMe$_3$)SiMe(OH)$_2$, for example, the O–H stretching vibration was found in the solid as a very broad band at 3350 cm^{-1}.[70] In subsequent single-crystal structure analyses of the silanols considered here, the presence of hydrogen bonds was confirmed.

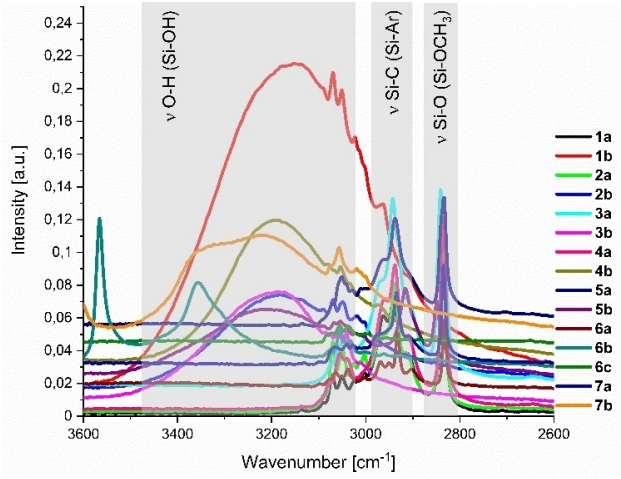

Figure 12. FTIR spectra of the synthesised compounds in the range of 2600 to 3600 cm^{-1}.

Single-crystal X-ray structures of the silanediols provide a deeper insight in the intermolecular interactions, especially with respect to the π-π interactions and the hydrogen bonding. Unfortunately, no single crystals of the only silanetriol could be obtained, but the high crystallinity of the compound was confirmed by X-ray powder diffraction. Table 3 summarizes the most important parameters. All parameters of the structure refinement can be found in the Supporting Information. The silanols considered crystallize mainly in a triclinic crystal system; only the compounds **1b** and **4b** crystallize in a monoclinic crystal system (Table 3). The loss of symmetry compared to the corresponding alkoxysilanes may be explained by the strong hydrogen bonds, as these determine the structure of the compounds.

The molecular structure of compound **1b** (Figure 13) shows comparable bond lengths and angles around the Si atom like the other structures studied (Table 1, Table 3), including the diphenylsilanediol known from the literature.[4] In the crystal structure compound **1b** is arranged in bilayers in which the hydroxyl groups face each other and form hydrogen bonds, with the hydrophobic phenyl and methyl groups also aligned with each other (Figure 13). The double layer structure resembles the structure of $C_6H_{11}Si(OH)_3$.[8] Generally, such double layer structures are more commonly found in silane triols.[8,19,31,32,68] Compound **1b** is the first example of a bilayer structure in a silanediol.[31,32] The two-dimensional structure is also reflected in the morphology of the platelet-shaped crystals.

When looking at the hydrophilic levels of the double layer structure, it is noticeable that they are always build from the

Table 3. Summary of important parameters of silanol crystal structures.

Compound	**1 b**	**2 b**[4]	**4 b**[a]	**5 b** (MeOH)	**5 b** (H_2O)	**5 b** (DCM)	**6 b**	**7 b**
Crystal system	monoclinic	triclinic	monoclinic	triclinic	triclinic	triclinic	triclinic	triclinic
Space group	$P2_1/c$	$P\bar{1}$	$P2_1/c$	$P\bar{1}$	$P\bar{1}$	$P\bar{1}$	$P\bar{1}$	$P\bar{1}$
d (Si–O_1) [pm]	164.05	164.86	171.26	163.59	164.33	163.87	163.29	164.02
d (Si–O_2) [pm]	164.02	163.87	164.59	164.21	163.44	163.58	164.19	164.18
d (Si–C_1) [pm]	185.91	186.48	187.44	186.03	185.67	185.84	186.82	185.40
d (Si–$C_{7/11/15/19}$) [pm]	184.12	185.28	185.83	185.90	185.58	185.79	187.00	186.64
∢ (Ar–Si–Ar) [°]	114.18	112.49	108.37	113.39	113.88	114.89	113.92	111.39
∢ (O–Si–O) [°]	110.11	109.81	108.39	107.00	110.34	109.00	111.30	109.80
$∢_{Tors}$ (Ar–Si–Ar) [°]	–	80.47	–	74.56	88.72	78.37	82.80	66.33
d (Si–OH) [pm]	164.05	163.87–164.86	164.59–171.16	163.59–164.21	163.63–163.91	163.58–163.87	163.29–164.19	164.02–164.18
d (O–H–O) [pm]	184.80–192.11	167.23–186.33	185.02–187.12	181.64–191.85	186.26–203.23	185.52–191.37	179.36–198.34	186.44–201.08
d (O–O) [pm]	266.96–273.10	268.78–277.15	271.29–273.25	264.85–278.39	265.64–282.57	268.10–273.26	264.73–279.98	269.21–282.23
∢ (O–H–O) [°]	164.90–174.92	156.05–169.51	164.07–167.75	163.53–176.29	137.53–168.08	156.80–175.81	169.61, 173.24	154.64–172.79
d (O–H–Ar) [pm]	–	–	–	–	–	312.83	–	–
Structure motif	double layer	linked hexamers	double layer	hexamers linked via solvent	hexamers linked via solvent	isolated octamers with hydrogen-bond-π interactions	isolated dimers	isolated tetramers of two dimers each

[a] The data obtained by single-crystal structure analysis of this compound were very poor. They were improved by powder diffraction of the same compound.

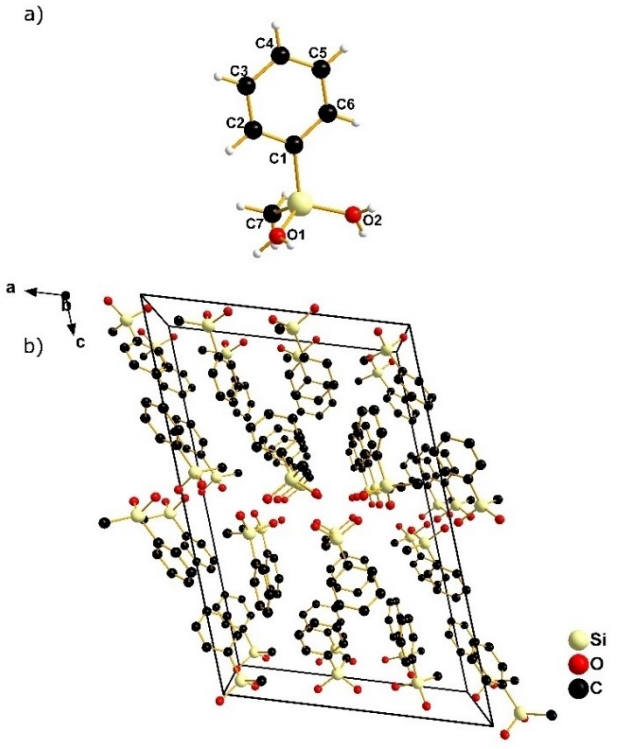

Figure 13. a) Single-crystal structure of compound **1 b** (CCDC 2093379). b) Illustration of the bilayer structure of compound **1 b** from a parallel view. When solving the single-crystal structure data, two half-occupied hydrogen atoms had to be bonded to an oxygen atom because domains with different orientations were present in the crystal.

same monomeric units linked by hydrogen bonds (Figure 14). It is composed of six molecules, essentially consisting of a tetrameric unit connected to another molecule on the outer sides in one direction by a hydrogen bond. Hydrogen bonds with different bond lengths (d (O–H···O): 184.80–192.11 pm) and angles (∢ (O-H···O): 164.90°–174.92°) could be observed. In turn, the two outer molecules are attached to the nearest monomeric unit. However, the tetramers are also bound to other tetramers in the b-direction forming alternating structures with eight- and six-membered rings.

Compound **2 b**[4] arranges itself into hexamers by hydrogen bonds. The different lengths of the hydrogen bonds indicate that a hexamer consists of two identical trimers. One such trimer is highlighted in Figure 15. The hexamers are linked together in a chain-like motif. The structure is referred to in the literature as "columns" consisting of hexamers. There is no linkage between the columns via hydrogen bonds.[4,31]

Very poor data were repeatedly obtained in the single-crystal structure analysis of compound **4 b**. The reason for this is that there are many layers growing on top of each other, resulting in a multiple twinned system. For this reason, this crystal structure was not registered in the Cambridge structural database. However, the connectivities were clearly visible, which makes a discussion of the general structure appropriate. However, discussions of exact bond angles or lengths should be treated with caution. Compound **4 b** shows a similar bonding situation as diphenylsilanediol.[4] The only exception is a larger Si–O bond length (Table 3), which can be based on strong hydrogen bonds or on the poor data quality. The latter was improved by X-ray powder diffraction of the compound. For this purpose, the poor single-crystal structure data were refined with a powder diffractogram of the same compound. We observed a platelet-like morphology of the crystals of compound **4 b**, which might be the result of a bilayer arrangement (Figure 16) as in compound **1 b**. It is feasible that a displacement between the hydrophobic aromatic units is rather simple, since

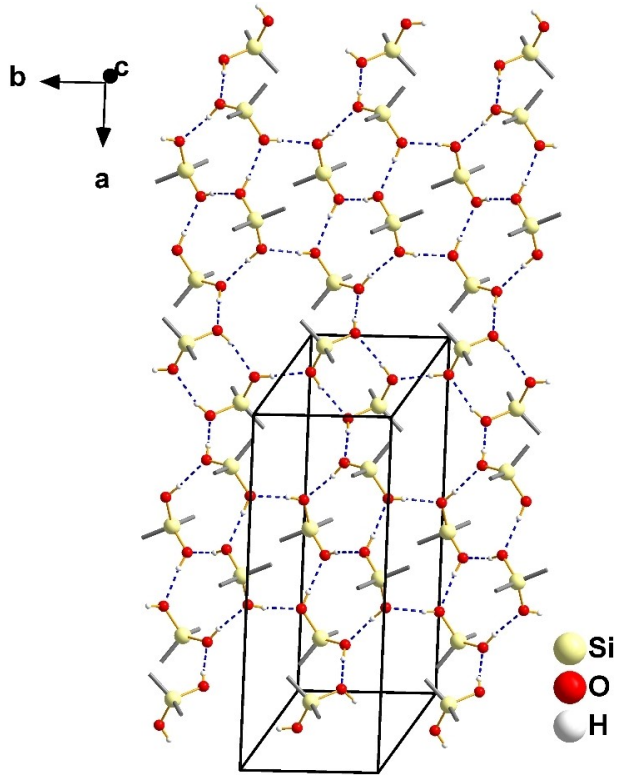

Figure 14. Illustration of a hydrogen bonded plane of compound **1 b** from vertical view. Hydrogen bonds are shown in blue. For the hydrogen atoms at the oxygen atoms, one orientation was chosen for this figure.

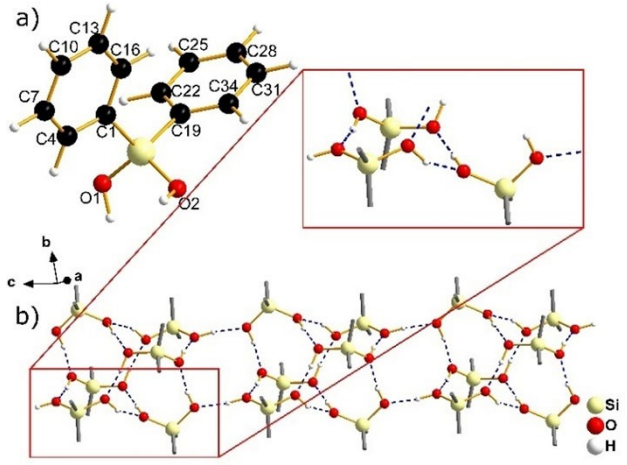

Figure 15. a) Single-crystal structure of compound **2 b**. b) Hexameric structure of diphenylsilanediol (**2 b**). Hydrogen bonds are coloured in blue.[4,71]

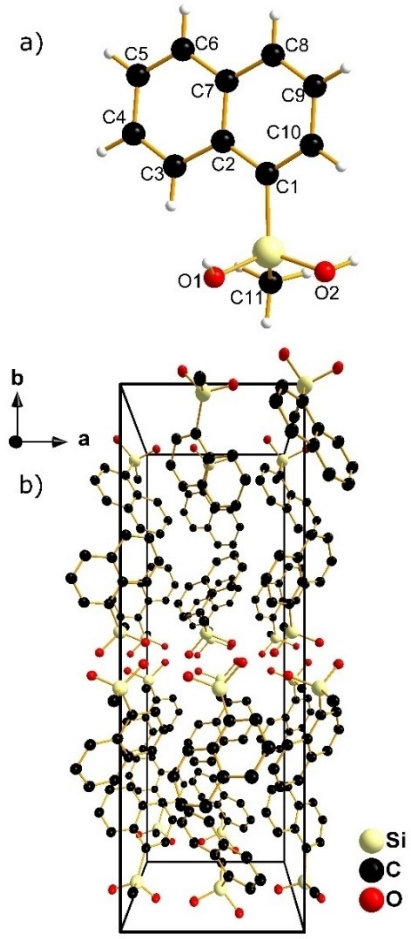

Figure 16. a) Single-crystal structure of compound **4 b**. b) Illustration of the bilayer structure of compound **4 b** from a parallel view.

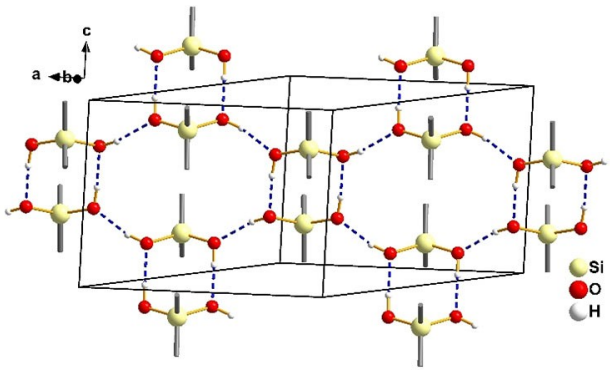

Figure 17. Hydrogen bonded plane structure of compound **4 b** from vertical view. Hydrogen bonds are coloured blue.

they are only subject to van der Waals interactions. A shift between the hydrophilic silanol groups is presumably much more difficult, since the strong hydrogen bonds would have to be cleaved for this.

In a vertical view of the planes of hydrogen bonded silanol groups, the plane consists of dimers, which in turn are bonded to other dimers by the two remaining unlinked hydrogen bond donors (Figure 17). This results in an interesting cross-shaped structure as a repeating unit. This structural motif has not yet been described for silanols.[31,32]

Single crystals of compound **5 b** could be obtained from three different solvents (methanol, ethyl acetate, and dichloromethane) (Table 3). The bond lengths and angles are similar to

diphenylsilanediol[4] and dimesitylsianediol.[72] The single-crystal structure of the crystal obtained from methanol showed a cage-like hexameric structure containing methanol molecules (Figure 18). The hexamers are linked together by two methanol molecules at a time. Different O–H···O bond lengths of 181.65 pm to 191.85 pm and different corresponding bond angles of 163.53° to 176.29° were found. Thus, different H-bridge bonds are present.

The structure of compound **5b**, which was obtained from a single crystal grown from ethyl acetate contains water molecules. This structure shows in principle the same motif as the one obtained from methanol (Figure 19). This also explains the similar lattice parameters of these two structures (Table 3). A linkage of the hexamers occurs by water molecules.

Crystallizing compound **5b** from dichloromethane leads to a different structure than that of methanol or ethyl acetate. Here, distorted dichloromethane molecules have been intercalated. In this structure, no linked cage-like hexamers are found as in the other two crystal structures of the compound (Figure 20). However, H-π interactions between a silanol group and a phenyl substituent of a different molecule can be observed within the octamers. The distance of the oxygen atom as hydrogen bond donor to the aromatic ring is 312.83 pm. This value is very close to a literature value (307 pm), which also describes the interaction of a hydroxyl group with an aromatic ring.[73] Different hydrogen bonds were again found with O–H···O bond lengths ranging from 185.52 pm to 191.37 pm and the corresponding bond angles ranging from 156.80° to 175.81°.

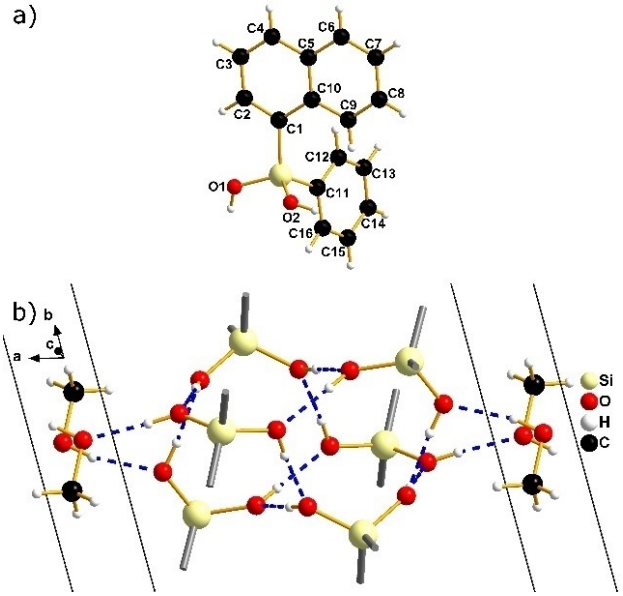

Figure 18. a) Single-crystal structure of compound **5b** (CCDC 2093381). b) Hexameric structure of compound **5b** crystallized from methanol, including hydrogen bonds coloured in blue.

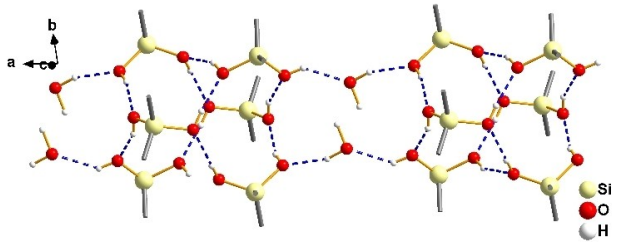

Figure 19. Hexameric structure of compound **5b** (CCDC 2093384) crystallized from ethyl acetate with water molecules intercalated into the crystal structure. Hydrogen bonds were coloured blue.

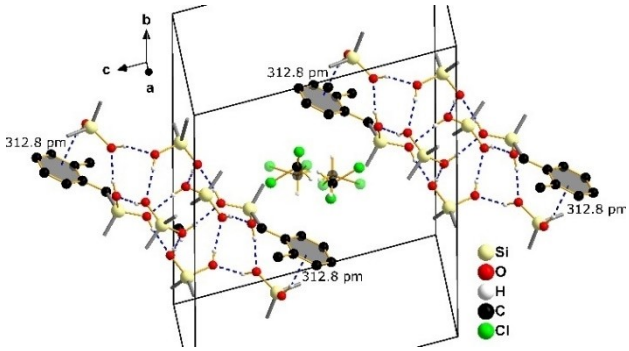

Figure 20. Octameric structure of compound **5b** (CCDC 2093387) crystallized from dichloromethane. Hydrogen bonds were coloured in blue. The transparent dichloromethane molecules are present at 40.9 % and the filled molecules at 59.1 %

The single-crystal structure of compound **6b** obtained here differs from known structures with respect to cell parameters, although structural parameters are almost identical.[74] The silanol **6b** was crystallized from tetrahydrofuran and shows formation of dimers, with two hydrogen bond donors saturated by THF molecules (Figure 21). However, unlike structures of the previous silanols, the dimers are not linked. This dimeric structure corresponds to structure type K from Figure 1.[32] Strong differences between the hydrogen bonds between the silanols and the hydrogen bonds between the silanols and THF are evident. Here, both the hydrogen bond lengths (O H···O), 179.36 pm and 198.34 pm, and the hydrogen bond angles, 169.61° and 173.24°, differ from each other (Table 3). This is easily understandable since the hydroxyl group of silanols and the ether group of THF differ significantly in their ability to act as hydrogen bond acceptors.

The bond lengths and angles of compound **7b** is very similar to the silanediols considered previously and also similar to diarylsilanediols known from literature such as diphenylsilanediol,[4] dimesitylsilanediol,[72] and di(naphthalen-1-yl)silanediol.[74] Silanol **7b** shows tetramer formation from two identical dimers (Figure 22). The two hydrogen bridge donors not involved in this are saturated by diethyl ether molecules, which in turn are disordered. One position of the diethyl ether molecules is present to 24.9 % and the other position to 75.1 %. However, as in compound **6b**, the tetramers are not connected. This structure corresponds to a section of structure type N (Figure 1). As with silanediol **6b** discussed previously, different hydrogen bonds are found here between the silanols and between the silanols and the incorporated diethyl ether

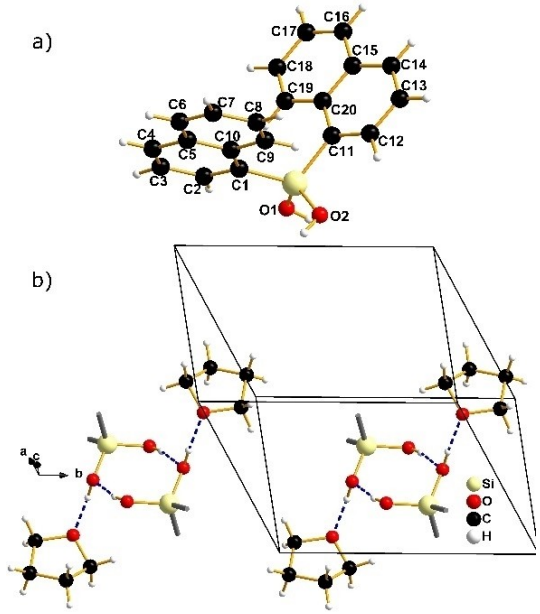

Figure 21. a) Single-crystal structure of compound **6b** (CCDC 2093390). b) Dimeric structure of compound **6b** crystallized from tetrahydrofuran. Hydrogen bonds are colored blue.

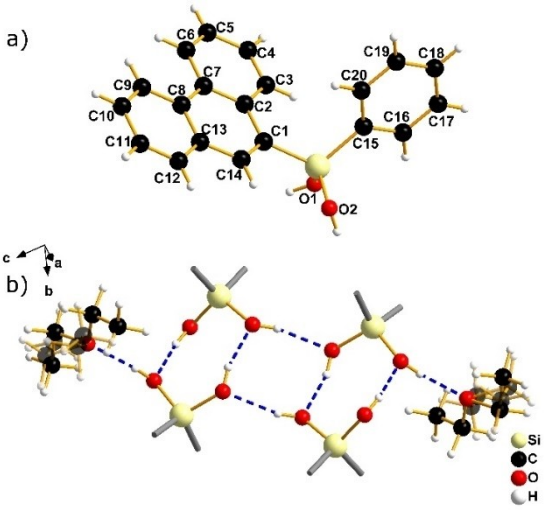

Figure 22. a) Single-crystal structure of compound **7b** (CCDC 2093392). b) Dimeric structure of compound **7b** crystallized from diethyl ether. Hydrogen bonds are coloured in blue. The transparent diethyl ether molecules are present at 24.9% and the filled molecules at 75.1%.

molecules. The hydrogen bond lengths here range from 186.44 pm to 201.08 pm and the hydrogen bond angles range from 154.64° to 172.79° (Table 3).

In summary, the X-ray single-crystal structures of silanols are dominated by strong hydrogen bonds. These stronger interactions substitute the π-π interactions found in the alkoxy and chlorosilanes. In the silanols, both the Ar–Si–Ar (108.37°–114.89°) and O–Si–O (107.00°–111.30°) angles and the torsion angles of the aromatic groups (66.33°–88.72°) do not follow any trend and are probably not related to the size of the substituents on the silicon atom. The bond angles are similar to those of the alkoxy or chlorosilanes. Based on the bond parameters of the hydrogen bonds, it can first be observed that the length of the Si–O bond hardly varies. The H···O distance varies more widely, ranging from 167.23 pm to 201.08 pm. The O···O distance is again less variable and ranges from 264.73 pm to 282.57 pm. The bond angle of the hydrogen bonds varies considerably from 136.23° to 176.29° and sometimes even within a compound. A comparison with values of compounds known from the literature shows almost no deviations.[4,8,31,75–77] Only the very small hydrogen bonding-angle of 136.23 ° in compound **5b** (H_2O) stands out. Compound **5b**, crystallized from dichloromethane, is noteworthy. The absence of a strong hydrogen bond acceptor allows the formation of hydrogen-bond π interactions with a spacing of 312.83 pm. A look at the structural motifs shows some correlation of these with the substituents attached to the silicon, which is also described in the literature.[31,32] The silanols with the most sterically demanding substituents, such as compounds **6b** and **7b** exhibit isolated and relatively small hydrogen bond complexes (dimer, tetramer). The sterically less demanding silanols show linked hexamers (**2b**, **5b** (MeOH), **5b** (H_2O)), octamers (**5b** (DCM)) or even infinite bilayer structures (**1b**, **4b**).

Conclusion

Nucleophilic substitution reactions of metalated 1-bromonaphthalene or 9-bromophenanthrene with tetramethoxysilane, methyltrimethoxysilane and phenyltrimethoxysilane result in the alkoxysilanes trimethoxy(naphthalen-1-yl)silane (**3a**), dimethoxy(methyl)(naphthalen-1-yl)silane (**4a**), dimethoxy-(naphthalen-1-yl)(phenyl)silane (**5a**), dimethoxydi(naphthalen-1-yl)silane (**6a**) and dimethoxy(phenanthren-9-yl)(phenyl)silane (**7a**). Lithiation of 1-bromonaphthalene by n-BuLi followed by reaction with tetrachlorosilane afforded dichlorodi(naphthalen-1-yl)silane (**6c**). Subsequently, hydrolysis of the above alkoxysilanes and commercially acquired dimethoxy(methyl)(phenyl) silane (1a) was carried out with acetic acid at different concentrations. Hydrolysis of dimethoxy(methyl)(phenyl)silane (**1a**) at 0 °C resulted in methyl(phenyl)silanediol (**1b**). Hydrolysis of trimethoxy(naphthalen-1-yl)silane (**3a**) at 0 °C yielded naphthalen-1-ylsilanetriol **(3b),** which could be insufficiently characterized by single-crystal X-ray structural analysis. A definite verification of the structure by spectroscopic methods was also not possible. Hydrolysis of dimethoxy(methyl)(naphthalen-1-yl) silane (**4a**) at 0 °C and room temperature gave methyl (naphthalen-1-yl)silanediol (**4b**). Hydrolysis of dimethoxy (naphthalen-1-yl)(phenyl)silane (**5a**) was realized at room temperature and afforded naphthalen-1-yl(phenyl)silanediol (**5b**). Phenanthren-9-yl(phenyl)silanediol (**7b**) was prepared by hydrolysis of dimethoxy(phenanthren-9-yl)(phenyl)silane (**7a**) at room temperature. The chlorosilane dichlorodi(naphthalen-1-yl) silane (**6c**) was hydrolyzed with water at room temperature to give di(naphthalen-1-yl)silanediol (**6b**). In general, all prepared compounds and additionally dimethoxy(methyl)(phenyl)silane (**1a**), dimethoxydiphenylsilane (**2a**) and diphenylsilanediol (**2b**)

were fully characterized. NMR spectroscopic studies showed hydrolysis of the methoxy groups to silanol groups depending on the reaction progress. The ^{29}Si NMR spectra of the alkoxysilanes and chlorosilane showed chemical shifts in the range from −52.78 ppm (trimethoxy(naphthalen-1-yl)silane (**3 a**)) to 7.62 ppm (dichlorodi(naphthalen-1-yl)silane (**6 c**)), which can be explained by the different electronic effects of the substituents. Also, the ^{29}Si NMR spectra of the studied silanols showed a large shift range from −61.78 ppm (naphthalen-1-ylsilanetriol (**3 b**)) to −18.85 ppm (methyl(naphthalen-1-yl) silanediol (**4 b**)). The alkoxysilanes were always more down-field shifted than their corresponding silanols. The chemical shifts of the silanol groups in the ^{1}H NMR spectra depend strongly on the solvent used. The silanol signals ranged across solvents from 5.44 ppm (methyl)(phenyl)silanediol (**1 b**) in acetone-d_6) to 7.42 ppm (di(naphthalen-1-yl)silanediol (**6 b**) in DMSO-d_6), which was attributed to the different ability to form hydrogen bonds with the solvent molecules. Comparison of the chemical shift of the silanol groups within a solvent did not show the same substituent effects as the ^{29}Si NMR signals. It can be assumed that the chemical shifts are also strongly influenced by the hydrogen bonds. ATR-FTIR spectroscopy was applied for reaction monitoring and could be used to distinguish the alkoxysilanes from the silanols by some vibrations, such as the O–H stretching vibration in the range of 3200 cm^{-1} or the Si–O stretching vibration of the Si–OMe functionality at about 2850 cm^{-1}. The strong shift of the previously mentioned O–H stretching vibration compared to literature values provided a first indication of strong hydrogen bonding in the solid. Single-crystal X-ray structure analyses of the compounds dimethoxy (naphthalen-1-yl)(phenyl)silane (**5 a**), dimethoxydi(naphthalen-1-yl)silane (**6 a**) and dimethoxy(phenanthren-9-yl)(phenyl)silane (**7 a**) showed Y-shaped-π-π interactions with a spacing from 485.1 pm (dimethoxy(phenanthren-9-yl)(phenyl)silane (**7 a**)) to 500.6 pm (dimethoxy(naphthalen-1-yl)(phenyl)silane (**5 a**)). The dichlorodi(naphthalen-1-yl)silane (**6 c**) was the only compound that showed a parallel-stacked-π-π interaction with a spacing of 392.2 pm. The crystal structures of the silanols exhibit strong hydrogen bonding patterns. The O–H–O distance ranges from 167.23 pm (diphenylsilanediol (**2 b**)) to 204.97 pm (naphthalen-1-yl(phenyl)silanediol (**5 b**)) and the bond angles of the hydrogen bonds range from 154.64° (phenanthrene-9-yl(phenyl) silanediol (**7 b**)) to 176.29° (naphthalen-1-yl(phenyl)silanediol (**5 b**)). Strongly different structural motifs were formed by the hydrogen bonds, including dimers (di(naphthalen-1-yl)silanediol (6b)), tetramers (phenanthren-9-yl(phenyl)silanediol (7b)), hexamers (diphenylsilanediol (2b) and naphthalen-1-yl(phenyl) silanediol (5b)), octamers (naphthalen-1-yl(phenyl)silanediol (5b)), and bilayer structures (methyl(phenyl)silanediol (1b) and methyl(naphthalen-1-yl)silanediol (4b)). These structural motifs are partly related to the steric repulsion of the substituents.

Experimental Section

Materials

Magnesium turnings (99.9%), toluene (for synthesis), acetic acid (99.8%), ethyl acetate (97%), diethyl ether (>99%), methanol (98% for synthesis), acetone (97% pract.), n-hexane (for synthesis), and ethanol (99% denatured with 1% PE) were purchased from central chemical storage of Saarland University. n-BuLi (2.5 M in hexane) and diphenylacetic acid (99+ %) were purchased from ACROS Organics (Geel, Belgium). 1-bromonaphthalene (97%), tetramethoxysilane (≥98%), phenylmethyldimethoxysilane (97%), triphenylchlorosilane (97%), and phenyltrimethoxysilane (97%) were purchased from ABCR GmbH (Karlsruhe, Germany). Methyltrimethoxysilane (97%), diphenylsilanediol (98%) and dimethoxydiphenylsilane (97%) were purchased from Alfa Aesar (Heysham, United Kingdom). Iodine (99.999%) were purchased from Merck KGaA (Darmstadt, Germany). absolute tetrahydrofuran, toluene, n-hexane, and diethyl ether were purified by Solvent Purification System (MBraun MB-SPS-800). Chloroform (≥99.8%), dichloromethane (99%), and tetrahydrofuran (≥99.5%) were purchased from Fisher Chemical (Hampton, USA). Acetonitrile (99%) was purchased from VWR Chemicals (Radnor, USA). Ammonium bicarbonate (p.a.) was purchased from Fluka (Buchs, Switzerland). Magnesium sulfate (99%) was purchased from Grüssing GmbH (Filsum, Germany). 9-Bromophenanthrene (99.83%) was purchased from BLDpharm (Shanghai, China).

Tetrachlorosilane (99%, Sigma-Aldrich, USA) was fractionally distilled before using as reactant.

All NMR spectra were recorded in acetone-d6 (99.8%, Deutero GmbH, Kastellaun, Germany), benzene-d_6 (99.0%, Deutero GmbH, Kastellaun, Germany), methanol-d_4 (99.80%, Eurisotope, Cambridge, United Kingdom), or DMSO-d_6 (99.8%, Deutero GmbH, Kastellaun, Germany).

All alkoxy and chlorosilane syntheses were carried out under an inert gas atmosphere using the Schlenk technique.

Characterization methods

ATR-FTIR spectra were measured on a Bruker Vertex 70 spectrometer at 4500–400 cm^{-1} with 4 cm^{-1} increment and 16 averaged scans. NMR spectra were obtained using a Bruker Avance III 400 MHz spectrometer at 400.13 MHz for ^{1}H NMR spectra, 79.49 MHz for ^{29}Si NMR spectra, and 100.62 MHz for ^{13}C NMR spectra and recorded using a Bruker Avance III 300 spectrometer at 300 MHz for ^{1}H NMR spectra, 59.60 MHz for ^{29}Si NMR spectra and 75.43 MHz for ^{13}C NMR spectra. The data set was collected using a Bruker X8 Apex diffractometer (2093379 (**1 b**), 2093384 (**5 b**), 2093387 (**5 b**), 2093388 (**5 a**), 2093389 (**6 a**), 2093390 (**6 b**), 2093392 (**7 b**) and 2073539 (**7 a**)) and a Bruker D8 Venture diffractometer with a microfocus sealed tube and a Photon II detector (2093381 (**5 b**)) at 140 K (2093390 (**6 b**)), 172 K (2073539 (**7 a**)) and 132 K (all other structures), respectively. Data were corrected for absorption effects using the multi-scan method. The structures were solved by direct methods using SHELXS-97 [1a] (2093384 (**5 b**), 2093387 (**5 b**), 2093389 (**6 a**), 2093390 (**6 b**) and 2073539 (**7 a**)) and SHELXT [1b] (2093379 (**1 b**), 2093381 (**5 b**), 2093388 (**5 a**), and 2093392 (**7 b**), respectively and were refined by full matrix least squares calculations on F2 (SHELXL2018 [2]) in the graphical user interface Shelxle [3]. All non H-atoms were located on the electron density maps and refined anisotropically. C-bound H atoms were placed in positions of optimized geometry and treated as riding atoms. Their isotropic displacement parameters were coupled to the corresponding carrier atoms by a factor of 1.2 (CH, CH2) or 1.5 (CH3).

The positional parameters of the O bonded H-atoms were refined using isotropic displacement parameters which were set at 1.5 times the Ueq value of the parent atom. Restraints of 0.84 (0.01) Å were used for the O–H bond lengths. Disorder: The solvent dichloromethylene was split over three positions (2093387 (**5b**)) and one diethyl ether (2093392 (**7b**)) was split over two positions. For the refinement of the disorder some DELU and SIMU restraints were applied in the refinement. Single-crystal X-ray diffraction:

Deposition Numbers 2093379 (for **1b**), 2093388 (for **5a**), 2093384 (for **5b**), 2093387 (for **5b**), 2093381 (for **5b**), 2093389 (for **6a**), 2093390 (for **6b**), 2073539 (for **7a**) and 2093392 (for **7b**) contain the supplementary crystallographic data for this paper. These data are provided free of charge by the joint Cambridge Crystallographic Data Centre and Fachinformationszentrum Karlsruhe Access Structures service. Powder diffractograms were determined by a Bruker D8 Advance diffractometer (Bruker AXS, Karlsruhe, Germany), with non-monochromatic Cu radiation, LynxEye 1D detector, in an angular range of 7–120° 2θ and a measurement time of 1 h. A step size of 0.013°, sample rotation of 0.5 rpm and 7x10 mm illuminated area were used. Powder diffractograms were analyzed using Topas 5.0 (Bruker AXS, Karlsruhe, Germany), with data fitted using a fundamental parameter approach. Raman spectra were recorded with a fiber-coupled Raman spectrometer (Horiba Scientific, Kyoto, Japan) using a 532 nm Nd:YAG laser, a "SuperHead" probe, and a sample chamber. The C, H, and N content of the compounds was determined using a Vario Micro cube (Elementar Analysensysteme GmbH, Langenselbold, Germany).

Synthetic Procedures

The synthesis procedures for all synthesized compounds are described below. The data for the characterization of the corresponding compounds can be found in Supporting Information.

The following alkoxysilanes (**3a**, **4a**, **5a**, **6a**, **7a**) were synthesized according to instructions known from the literature.[78,79]

Trimethoxy(naphthalen-1-yl)silane (**3a**), dimethoxy (methyl)(naphthalen-1-yl)silane (**4a**), dimethoxy(naphthalen-1-yl)(-phenyl)silane (**5a**) and dimethoxydi(naphthalen-1-yl)silane (**6a**)

All four compounds were synthesized in a similar manner. A general procedure follows, and the amounts used can be found in Table 4. A spatula tip of iodine and the appropriate amounts of magnesium turnings, absolute tetrahydrofuran, and the appropriate silane component (tetramethoxysilane, methyltrimethoxysilane, or phenyltrimethoxysilane) were added to a heated and argon-purged three-necked flask with a dropping funnel and reflux condenser under argon atmosphere. The mixture was heated to 35 °C. Then, the appropriate amount of 1-bromonaphthalene was added over 20–30 min at 35 °C with stirring. Subsequently, the mixture was first heated to 50 °C for 1 h and then to 75 °C for another hour. Subsequently, it was cooled to room temperature and stirred overnight. For workup, the reaction solution was carefully decanted to condense on the rotary evaporator without magnesium residue. The residue after evaporation was taken up in 200 mL of hexane, heated to boiling for about 5 min, and filtered after cooling. The filtration cake was again taken up in 150 mL of hexane and again heated to boiling for about 5 min and also filtered after cooling. The combined filtrates were concentrated. This gave a colourless liquid in the case of Trimethoxy(naphthalen-1-yl)silane (**3a**) and dimethoxy(methyl)-(naphthalen-1-yl)silane (**4a**), a yellow liquid in the case of dimethoxy(naphthalen-1-yl)(phenyl)silane (**5a**), and a white solid in the case of dimethoxydi(naphthalen-1-yl)silane (**6a**). The liquid products were distilled for further purification at 0.05 mbar (boiling point (**3a**): 130 °C; boiling point (**4a**): 120 °C; boiling point (**5a**): 140 °C). The white solid was washed several times with cold hexane for further purification. The Trimethoxy (naphthalen-1-yl)silane (**3a**) and dimethoxy(naphthalen-1-yl)(phenyl)silane (**5a**) solidified to a solid overnight. The corresponding yields are 76.7 % for **3a**, 92.1 % for **4a**, 81.2 % for **5a**, and 43.8 % for **6a**. Crystals for single-crystal structure analysis could be obtained directly for compound **3a**, where the single-crystal structure was already available in the working group. For compound **5a**, crystals were obtained by slow evaporation of a saturated solution in methanol.

Table 4. Quantities for the syntheses of compounds **3a**, **4a**, **5a**, **6a**.

Substance	mass [g]	volume [mL]	mole [mmol]	equivalents
Trimethoxy(naphthalen-1-yl)silane (**3a**)				
Mg turnings	2.937	–	120.84	1.5
1-bromo-naphthalene	16.575	11.2	80.05	1.0
tetramethoxysilane	37.080	36.0	243.59	3.0
THF (abs.)	–	130.0	–	–
Dimethoxy(methyl)(naphthalen-1-yl)silane (**4a**)				
Mg turnings	3.140	–	129.19	1.5
1-bromonaphthalene	17.760	12.0	85.77	1.0
methyltrimethoxysilane	35.520	37.0	260.75	3.0
THF (abs.)	–	140.0	–	–
Dimethoxy(naphthalen-1-yl)(phenyl)silane (**5a**)				
Mg turnings	4.340	–	178.60	1.5
1-bromonaphthalene	24.420	16.5	117.90	1.0
phenyltrimethoxysilane	70.090	66.0	353.50	4.0
THF (abs.)	–	200.0	–	–
Dimethoxydi(naphthalen-1-yl)silane (**6a**)				
Mg turnings	4.234	–	174.20	2.8
1-bromonaphthalene	24.042	16.2	116.11	1.8
tetramethoxysilane	9.579	9.3	62.93	1.0
THF (abs.)	–	100.0	–	–

Dimethoxy(phenanthren-9-yl)(phenyl)silane (**7a**): In a 500 mL three-necked flask with dropping funnel and reflux condenser with gas connection, 4.2955 g (176.73 mmol) of magnesium turnings and 160 mL of absolute tetrahydrofuran were added and heated to 40 °C under an argon atmosphere. Subsequently, 29.8622 g (116.14 mmol) of 9 bromophenanthrene was dissolved in 30 mL of absolute THF in a dropping funnel, added over approximately 30 min at 40 °C with stirring, and then heated for approximately 2.5 h with reflux. To a second, also inert, 500 mL three-necked flask with a gas connection was added 67.7 mL (362.65 mmol) phenyltrimethoxysilane and cooled to approximately −30 °C using an ethyl acetate/N_2 cold bath. Then, the still hot reaction solution without the remaining magnesium was added quickly to the phenyltrimethoxysilane using a cannula. After the reaction solution was stirred in the cooling bath for 1 h, the same was replaced by an ice bath and stirred overnight, allowing the solution to warm to room temperature. The reaction solution was transferred to a 500 mL round bottom flask and concentrated on the rotary evaporator as much as possible. To the residue was added 200 mL of n-hexane, heated to boiling for about 10 minutes, and filtered. This residue was again taken up in 100 mL of n-hexane, heated to boiling for about 10 minutes, and hot filtered, with an initial portion of the product already crystallized out in the suction flask. The combined filtrates were concentrated as much as possible on the rotary evaporator and placed in the freezer overnight at −25 °C to crystallize the remaining product. The mixture was then filtered and the residue, as well as the previously crystallized solid, was washed with cold methanol. A white crystalline solid (66.3 %) was obtained.

Dichlorodi(naphthalen-1-yl)silane (**6c**): The chlorosilane **6c** was synthesized following the literature.[49] To a flask fitted with a dropping funnel, 20.72 g (100.0 mmol) of 1-bromonaphthalene in

140 mL Et_2O was added. 44 mL (110.0 mmol) of n-BuLi in 40 mL Et_2O was added dropwise at −78 °C. After addition, the reaction was kept at −78 °C for 10 min and then brought to room temperature and stirred for 30 min. The solution was added via a cannula to a solution of 5.75 mL (50 mmol) $SiCl_4$ in 120 mL Et_2O at 0 °C. The reaction was stirred for 2 h and then warmed to room temperature. The solvent was removed under reduced pressure and the residue was dissolved in boiling toluene. Insoluble salts were removed by filtration through Cellite and washed with hot toluene. The solvent from the resulting clear solution was removed under reduced pressure, followed by purification by recrystallization from toluene. **6c** was obtained as crystalline material in a yield of 65.9%. Crystals suitable for X-ray diffraction analysis could be grown from toluene at room temperature.

All the syntheses of the following silanols starting from the alkoxysilanes (**1b**, **3b**, **4b**, **5b**, **7b**) were carried out following the literature.[80]

Methyl(phenyl)silanediol (**1b**): To a snap cap glass with stirrer, 0.6 mL of distilled water and 11.4 μL of 50 wt% acetic acid were added. The reaction mixture was cooled in an ice bath. Then, 0.73 g (4.00 mmol) of dimethoxy(methyl)(phenyl)silane (**1a**) was added in portions over 30 min and stirred for 2 h in an ice bath. The water and acetic acid were then removed rapidly under high vacuum. The white solid was washed several times with cold toluene. The product (white solid) was dried under high vacuum. A yield of 40.1% was obtained. Crystals suitable for single-crystal structure analysis could be obtained by evaporating a saturated solution in acetone.

Naphthalen-1-ylsilanetriol (**3b**): To a snap cap glass with stirrer, 2.0 mL of distilled water and 59 μL of 50 wt% acetic acid were added and cooled in an ice bath. Then 0.5 g (2.01 mmol) of Trimethoxy(naphthalen-1-yl)silane (**3a**) was added in portions over 30 min and stirred for 2 h in an ice bath. A new ice bath was then prepared and the reaction mixture was stirred for 18 h, without continuous maintenance of cooling. The white precipitate was cold filtered off and washed several times with cold toluene. The product (white solid) was dried under high vacuum. A yield of 75.8% was obtained.

Methyl(naphthalen-1-yl)silanediol (**4b**): To a snap cap glass with stirrer, 284 μL distilled water and 32 μL 50 wt% acetic acid were added. The reaction mixture was cooled in an ice bath. Then, 0.465 g (2.00 mmol) of Dimethoxy(methyl)(naphthalen-1-yl)silane (**4a**) was added in portions over 30 min and stirred for 2 h in an ice bath. This was followed by stirring with a new ice bath for 20 h, at which time the ice bath thawed completely. The white precipitate was cold filtered off and washed several times with cold toluene. The product (white solid) was dried under high vacuum. A yield of 66.0% was obtained. Crystals for single-crystal structure analysis could be obtained by slow evaporation of a saturated solution of the compound in DCM.

Naphthalen-1-yl(phenyl)silanediol (**5b**): To a snap cap glass with a stirrer, 2.0 mL of distilled water and 1.27 mL of 99 wt% acetic acid were added. Then 0.588 g (2.00 mmol) of Dimethoxy(naphthalen-1-yl)(phenyl)silane (**5a**) was added in portions over 30 min and stirred for 20 h at room temperature. The white precipitate was filtered off and washed several times with cold toluene. The product (white solid) was dried under high vacuum. A yield of 60.3% was obtained. Crystals for single-crystal structure analysis could be obtained from methanol, ethyl acetate or DCM.

Di(naphthalen-1-yl)silanediol (**6b**): Silanediol **6b** was synthesized following the literature.[31,81,82] To a solution of 0.9488 g (12.00 mmol) ammonium bicarbonate in 40 mL water, overlaid with 40 mL diethyl ether, was added a solution of 2.0 g (5.68 mmol) dichlorodi(naphthalen-1-yl)silane (**6c**) in 100 mL diethyl ether with stirring at room temperature. The reaction mixture was stirred for an additional 2 h at room temperature. The ether phase was separated, washed with water, and dried over magnesium sulphate. The product was isolated by removing the ether. A nearly quantitative yield (about 99%) was obtained. Single crystals, which were suitable for analysis, could be obtained from a solution in THF.

Phenanthren-9-yl(phenyl)silanediol (**7b**): To a snap cap glass with a stirrer, 2.0 mL of distilled water and 4.444 mL of 99 wt% acetic acid were added. Then 0.689 g (2.00 mmol) of Dimethoxy(phenanthren-9-yl)(phenyl)silane (**7a**) was added in portions over 30 min and stirred for 20 h at room temperature. The white precipitate was filtered off and washed several times with cold toluene. The product (white solid) was dried under high vacuum. A yield of 59.0% was obtained. Crystals for single-crystal structure analysis could be obtained from a solution in diethyl ether by evaporation.

Acknowledgements

Instrumentation and technical assistance for this work were provided by the Service Center X-ray Diffraction, with financial support from Saarland University and German Science Foundation (project numbers INST 256/506-1, INST 256/349-1). Open Access funding enabled and organized by Projekt DEAL.

Conflict of Interest

The authors declare no conflict of interest.

Keywords: Alkoxysilanes · H-bond structural motifs · Hydrolysis · ^{29}Si NMR · Organosilanols

[1] A. Ladenburg, *Ann. Chem. Pharm.* **1871**, *4*, 901–903.
[2] M. Kakudo, T. Watase, *J. Chem. Phys.* **1953**, *21*, 167–168.
[3] N. Kasai, M. Kakudo, *Bull. Chem. Soc. Jpn.* **1954**, *27*, 605–608.
[4] J. K. Fawcett, R. June, *Can. J. Chem.* **1977**, *55*, 3631–3635.
[5] W. T. Grubb, **1954**, *76*, 3408–3414.
[6] G. Schott, H. Berge, *Z. Anorg. Allg. Chem.* **1958**, *297*, 32–43.
[7] T. Takiguchi, *J. Am. Chem. Soc.* **1959**, *81*, 2359–2361.
[8] H. Ishida, J. L. Koenig, K. C. Gardner, *J. Chem. Phys.* **1982**, *77*, 5748–5751.
[9] L. J. Tyler, *J. Am. Chem. Soc.* **1954**, *77*, 770–771.
[10] J. Curtice, H. Gilman, G. S. Hammond, *J. Am. Chem. Soc.* **1957**, *79*, 4754–4759.
[11] L. Tong, Y. Feng, X. Sun, Y. Han, D. Jiao, X. Tan, *Polym. Adv. Technol.* **2018**, *29*, 2245–2252.
[12] M. Zhao, Y. Feng, Y. Li, G. Li, Y. Wang, Y. Han, X. Sun, X. Tan, *J. Macromol. Sci. Part A Pure Appl. Chem.* **2014**, *51*, 653–658.
[13] J. S. Kim, S. Yang, B. S. Bae, *Chem. Mater.* **2010**, *22*, 3549–3555.
[14] M. Chen, G. Zhang, X. Liang, W. Zhang, L. Zhou, B. He, P. Song, X. Yuan, C. Zhang, L. Zhang, H. Yu, H. Yang, *RSC Adv.* **2016**, *6*, 70825–70831.
[15] S. Yang, S. Y. Kwak, J. Jin, J. S. Kim, Y. Choi, K. W. Paik, B. S. Bae, *J. Mater. Chem.* **2012**, *22*, 8874–8880.
[16] Y. H. Kim, J. Y. Bae, J. Jin, B. S. Bae, *ACS Appl. Mater. Interfaces* **2014**, *6*, 3115–3121.
[17] S. Spirk, M. Nieger, R. Pietschnig, *Dalton Trans.* **2009**, *596*, 163–167.
[18] N. Hurkes, C. Bruhn, F. Belaj, R. Pietschnig, *Organometallics* **2014**, *33*, 7299–7306.
[19] N. Hurkes, H. M. A. Ehmann, M. List, S. Spirk, M. Bussiek, F. Belaj, R. Pietschnig, *Chem. Eur. J.* **2014**, *20*, 9330–9335.
[20] M. W. Mutahi, T. Nittoli, L. Guo, S. M. N. Sieburth, *J. Am. Chem. Soc.* **2002**, *124*, 7363–7375.

[21] C. A. Chen, S. M. N. Sieburth, A. Glekas, G. W. Hewitt, G. L. Trainor, S. Erickson-Viitanen, S. S. Garber, B. Cordova, S. Jeffry, R. M. Klabe, *Chem. Biol.* **2001**, *8*, 1161–1166.
[22] S. E. Denmark, A. Ambrosi, *Org. Process Res. Dev.* **2015**, *19*, 982–994.
[23] S. E. Denmark, R. F. Sweis, *Acc. Chem. Res.* **2002**, *35*, 835–846.
[24] S. I. Kondo, Y. Bie, M. Yamamura, *Org. Lett.* **2013**, *15*, 520–523.
[25] R. Pietschnig, in *Main Gr. Strateg. Towar. Funct. Hybrid Mater.*, **2017**, pp. 141–162.
[26] S. Spirk, H. M. Ehmann, R. Kargl, N. Hurkes, M. Reischl, J. Novak, R. Resel, M. Wu, R. Pietschnig, V. Ribitsch, *ACS Appl. Mater. Interfaces* **2010**, *2*, 2956–2962.
[27] J. Escorihuela, H. Zuilhof, *J. Am. Chem. Soc.* **2017**, *139*, 5870–5876.
[28] D. W. Lee, B. R. Yoo, *J. Ind. Eng. Chem.* **2016**, *38*, 1–12.
[29] B. R. Yoo, D. E. Jung, J. S. Han, *Mater. Res. Soc. Symp. Proc.* **2009**, *1174*.
[30] R. Pietschnig, S. Spirk, *Coord. Chem. Rev.* **2016**, *323*, 87–106.
[31] P. D. Lickiss, *Adv. Inorg. Chem.* **1995**, *42*, 147–262.
[32] V. Chandrasekhar, R. Boomishankar, S. Nagendran, *Chem. Rev.* **2004**, *104*, 5847–5910.
[33] O. M. Steward, D. R. Fussaro, *J. Organomet. Chem.* **1977**, *120*, C28–C32.
[34] C. Eaborn, W. A. Stańczyk, *J. Chem. Soc. Perkin Trans. II* **1984**, 2099–2103.
[35] K. Krekic, N. F. Hurkes, C. Bruhn, F. Belaj, R. Pietschnig, *Z. Anorg. Allg. Chem.* **2016**, *642*, 302–305.
[36] S. Spirk, F. Belaj, J. Baumgartner, R. Pietschnig, *Z. Anorg. Allg. Chem.* **2009**, *635*, 1048–1053.
[37] P. Jutzi, M. Schneider, H. G. Stammler, B. Neumann, *Organometallics* **1997**, *16*, 5377–5380.
[38] Z. H. Aiube, N. H. Buttrus, C. Eaborn, P. B. Hitchcock, J. A. Zora, *J. Organomet. Chem.* **1985**, *292*, 177–188.
[39] S. S. Al-Juaid, C. Eaborn, P. B. Hitchcock, P. D. Lickiss, A. Möhrke, P. Jutzi, *J. Organomet. Chem.* **1990**, *384*, 33–40.
[40] S. Spirk, S. Salentinig, K. Zangger, F. Belaj, R. Pietschnig, *Supramol. Chem.* **2011**, *23*, 801–805.
[41] S. Spirk, R. J. F. Berger, C. G. Reuter, R. Pietschnig, N. W. Mitzel, *Dalton Trans.* **2012**, *41*, 3630–3632.
[42] N. Hurkes, S. Spirk, F. Belaj, R. Pietschnig, *Z. Anorg. Allg. Chem.* **2013**, *639*, 2631–2636.
[43] J. O. Bauer, *Z. Anorg. Allg. Chem.* **2021**, *647*, 1–6.
[44] E. C. Lee, D. Kim, P. Jurečka, P. Tarakeshwar, P. Hobza, K. S. Kim, *J. Phys. Chem. A* **2007**, *111*, 3446–3457.
[45] C. R. Martinez, B. L. Iverson, *Chem. Sci.* **2012**, *3*, 2191–2201.
[46] Y. M. Lim, M. E. Lee, U. Lee, *Bull. Korean Chem. Soc.* **2010**, *31*, 216–219.
[47] R. Fritzsche, F. Seidel, T. Rüffer, R. Buschbeck, A. Jakob, H. Freitag, D. R. T. Zahn, H. Lang, M. Mehring, *J. Organomet. Chem.* **2014**, *755*, 86–92.
[48] C. A. Hunter, J. K. M. Sanders, *J. Am. Chem. Soc.* **1990**, *112*, 5525–5534.
[49] J. Binder, PhD Thesis, Graz University of Technology (AT), **2015**.
[50] J. Binder, R. C. Fischer, M. Flock, A. Torvisco, F. Uhlig, *Phosphorus Sulfur Silicon Relat. Elem.* **2015**, *190*, 1980–1993.
[51] J. Binder, R. C. Fischer, M. Flock, H. G. Stammler, A. Torvisco, F. Uhlig, *Phosphorus Sulfur Silicon Relat. Elem.* **2016**, *191*, 478–487.
[52] S. Altmann, J. Pfeiffer, *Monatsh. Chem.* **2003**, *134*, 1081–1092.
[53] B. Tan, S. E. Rankin, *J. Phys. Chem. B* **2006**, *110*, 22353–22364.
[54] F. D. Osterholtz, E. R. Pohl, *J. Adhes. Sci. Technol.* **1992**, *6*, 127–149.
[55] D. E. Leyden, J. B. Atwater, *J. Adhes. Sci. Technol.* **1991**, *5*, 815–829.
[56] E. Liepiņš, I. Zicmane, E. Lukevics, *J. Organomet. Chem.* **1986**, *306*, 167–182.
[57] M. Unno, T. Tanaka, H. Matsumoto, *J. Organomet. Chem.* **2003**, *686*, 175–182.
[58] R. J. Hook, *J. Non-Cryst. Solids* **1996**, *195*, 1–15.
[59] J. C. Echeverría, P. Moriones, G. Arzamendi, J. J. Garrido, M. J. Gil, A. Cornejo, V. Martínez-Merino, *J. Sol-Gel Sci. Technol.* **2018**, *86*, 316–328.
[60] S. C. C. van der Lubbe, C. Fonseca Guerra, *Chem. Asian J.* **2019**, *14*, 2760–2769.
[61] K. H. Scheit, *Angew. Chem.* **1967**, *4*, 190.
[62] R. West, R. H. Baney, *J. Am. Chem. Soc.* **1959**, *81*, 6145–6148.
[63] C. Laurence, M. Berthelot, *Perspect. Drug Discovery Des.* **2000**, *18*, 39–60.
[64] Y. S. Li, Y. Wang, S. Ceesay, *Spectrochim. Acta Part A* **2009**, *71*, 1819–1824.
[65] I. S. Ignatyev, F. Partal, J. J. L. González, T. Sundius, **2004**, *60*, 1169–1178.
[66] W. E. Newton, E. G. Rochow, *J. Chem. Soc. A* **1970**, 2664–2668.
[67] X. Chen, D. Eldred, J. Liu, H. Chiang, X. Wang, M. A. Rickard, S. Tu, L. Cui, P. LaBeaume, K. Skinner, *Appl. Spectrosc.* **2018**, *72*, 1404–1415.
[68] L. D. Cother, PhD Thesis, Imperial College London (UK), **1998**.
[69] U. B. Mioč, L. J. Bogunović, S. V. Ribnikar, M. D. Dragojević, *J. Mol. Struct.* **1988**, *177*, 379–383.
[70] V. Chandrasekhar, S. Nagendran, R. J. Butcher, *Organometallics* **1999**, *18*, 4488–4492.
[71] L. Parkanyi, G. Bocelli, *Cryst. Struct. Commun.* **1978**, *7*.
[72] N. T. Tran, T. Min, A. K. Franz, *Chem. Eur. J.* **2011**, *17*, 9897–9900.
[73] A. T. McPhail, G. A. Sim, *Chem. Commun.* **1965**, *7*, 124–126.
[74] N. T. Tran, S. O. Wilson, A. K. Franz, *Org. Lett.* **2012**, *14*, 186–189.
[75] N. H. Buttrus, C. Eaborn, A. D. Taylor, P. B. Hitchcock, P. D. Lickiss, *J. Organomet. Chem.* **1986**, *309*, 25–33.
[76] O. Graalmann, U. Klingebiel, W. Clegg, M. Haase, G. M. Sheldrick, *Chem. Ber.* **1984**, *117*, 2988–2997.
[77] S. S. Al-Juaid, C. Eaborn, P. B. Hitchcock, P. D. Lickiss, *J. Organomet. Chem.* **1989**, *362*, 17–22.
[78] H. Wei, P. Bichen, X. Yang, Y. Youxue, Z. Ying, Z. Xiaojuan, *CN104788488 A*, **2015**.
[79] K. Shuto, T. Kato, T. Nagasawa, *PCT/JP2017/017582*, **2017**.
[80] K. S. Lokare, N. Frank, B. Braun-cula, I. Goikoetxea, J. Sauer, C. Limberg, *Angew. Chem. Int. Ed.* **2016**, *55*, 12325–12329; *Angew. Chem.* **2016**, *128*, 12513–12517.
[81] G. Schott, W. D. Sprung, *Z. Anorg. Allg. Chem.* **1964**, *333*, 76–89.
[82] P. Voss, C. Meinicke, E. Popowski, H. Kelling, *J. Prakt. Chem.* **1978**, *320*, 34–42.

Manuscript received: July 27, 2021
Accepted manuscript online: September 21, 2021
Version of record online: October 21, 2021

